C Journal of Carbon Research

MDPI

Article

Joule Heating of Carbon-Based Materials Obtained by Carbonization of *Para*-Aramid Fabrics

Daniel Karthik *, Jiri Militky, Yuanfeng Wang and Mohanapriya Venkataraman

Department of Material Engineering, Technical University of Liberec, Studentska 1402/2, 46117 Liberec, Czech Republic

* Correspondence: daniel.karthik@tul.cz

Abstract: The Joule heating behavior of carbon-based materials obtained by the process of carbonization of industrial para-aramid fabric wastes are investigated in the present work. Carbonization involves a process of thermally decomposing organic material, thereby altering its physical and chemical properties to obtain carbon-rich materials that are electrically conductive and display Joule heating behavior. The principle of Joule heating is based on the intrinsic electrical resistance of the material across an applied voltage. Here, para-aramid woven fabric wastes are converted into activated carbon materials through straightforward, controlled, single-step thermal treatments by three different kinds of atmosphere, i.e., in the CO_2 evolved from charcoal, a mixture of gases from ammonium bicarbonate salt (NH_4HCO_3), and Nitrogen gas (N_2), respectively, inside a high-temperature furnace. The carbonization temperatures were varied from 800 to 1100 °C. The carbonization process variables were optimized to obtain carbon-rich materials with lower electrical resistivity. The results of electrical resistivity measurements show that for all three methods, the electrical resistivity decreases with increasing carbonization temperatures. An experimental setup consisting of an infrared (IR) camera, positioned over the surface of the fabric specimen to record the surface temperature of the material connected to a DC power supply, was employed. The kinetics of Joule heating and subsequent cooling were also analyzed at a fixed voltage of 5 V by recording the changes in surface temperature with respect to time. The heating–cooling cycle is described by a simple kinetic model of first order.

Keywords: Joule heating; carbonization; activated carbon; electrical resistivity; para-aramid wastes

Citation: Karthik, D.; Militky, J.; Wang, Y.; Venkataraman, M. Joule Heating of Carbon-Based Materials Obtained by Carbonization of *Para*-Aramid Fabrics. *C* **2023**, *9*, 23. https://doi.org/10.3390/c9010023

Academic Editor: Gil Gonçalves

Received: 12 January 2023
Revised: 10 February 2023
Accepted: 13 February 2023
Published: 15 February 2023

1. Introduction

In recent years, the growing demand for more multi-functional, techno-economic and sustainable materials for various applications has attracted enormous research interest. Electrothermal and Ohmic heating performance of textiles in particular have compelled much attention in various heating applications. Carbonaceous materials in various forms (fibers, fabrics, or particles) have drawn considerable attention as effective heating elements due to their intrinsic thermal and electrical properties [1,2]. These materials have versatile applications in areas such as smart sensors, grounding materials to dissipate static charge, structural health monitoring, de-icing in aerospace and wind-turbine structures, and electromagnetic interference (EMI) shielding materials, among others [3–6].

Joule heating (also referred to as Ohmic heating or resistive heating), based on the law of conservation of energy, is a phenomenon that occurs when a voltage difference is applied across a conductive material such that electrical energy is consumed in overcoming the resistance in the material between the electrons and the atoms, causing this energy to be generated in the form of heat. This heating is referred to as Joule's effect. The amount of heat produced by the material is proportional to the square of the current, the resistance of the circuit, and the duration for which the current flows through the circuit [7], shown mathematically as follows:

$$Q = I^2Rt \quad (1)$$

where Q is the heat produced by the material in joules; I is the electrical current flowing through the conductor, in amperes; R is the electrical resistance, in ohms; t is the elapsed time, in seconds. Joule heating has been extensively used in various applications where thermal energy produced by the resistance in the conductor is put to use in the form of conduction, convection, or radiation.

It is quite rhetorical to query how the processes of pyrolysis and carbonization of various polymeric materials have been constantly carried out over time, in order to obtain carbon-rich products conducive to various areas of application. Thermal decomposition through these two phases involves aromatic evolution and polymerization of the organic material, through bond cleavage reactions and the rearrangement of compounds in an inert atmosphere over a wide temperature range [8–12]. Non-carbon volatiles in the form of nitrogen, hydrogen, methane, carbon dioxide, carbon monoxide, ammonia, water, etc., are eliminated during the process of carbonization, which contributes to almost 50 percent or more by weight of the precursor material. The maximum temperature of carbonization depends on the required type of carbon and its specific application. Fundamental modifications can be observed in the chemical composition as well as the physical properties [13–17].

The type of the precursor and the selected process parameters greatly influence the final product of carbonization. Having said that, para-aramids (1, 4 p-phenylene terephthalamide), more commonly recognized as Kevlar, have shown to be suitable precursors to obtain carbon fibers by various methods of carbonization and activation (physical and chemical) [10,18,19]. The carbonaceous materials obtained displayed significant electrical and thermal properties. In the present experiment, we utilized feedstock material, gathered from a local industry, as Kevlar fabric wastes and carbonized them to obtain carbon fabric produce.

In the present study, a comparative analysis of the Ohmic heating behavior and electrical properties of carbon fabrics obtained by the carbonization of para-aramid fabrics by three different procedures was conducted. Here, we utilize charcoal and ammonium bicarbonate salt (in separate methods), which are inexpensive and commonly available, in comparison to N_2 gas, in order to potentially create an oxygen-free atmosphere inside the furnace to support activation during the carbonization process. The electrical resistivity and Joule heating behavior of the activated carbon are analyzed. A kinetics model is further used to analyze the heating and cooling cycles of the Joule-heated materials with respect to voltage and time. The para-aramid fabrics used for this study were industrial feedstock material, hence contributing towards sustainability and the potential utilization of textile wastes.

2. Experimental

2.1. Materials

Kevlar 29 para-aramid woven fabric was obtained from Veba Textile Mills Ltd. (Broumov), Czech Republic, in the form of discarded short fabric wastes with a yarn count of 1710 dtex, density of 1.43 g/cm^3, and 5.2 wt % moisture content (parameters specified by the manufacturing company).

2.2. Methodology

Carbonization of Kevlar was carried out using three different methods based on the atmosphere created in the furnace during the process of pyrolysis, as described below.

Method 1: Charcoal Method

The carbonization of Kevlar fibrous wastes was carried out under the layer of charcoal, creating a CO_2 atmosphere, in a high-temperature furnace. The Kevlar fabric was directly carbonized without any intermediate stabilization step. The final temperatures of 800 °C, 900 °C, 1000 °C, and 1100 °C, with heating rate of 300 °C/h and without any holding time, were adopted during the process of carbonization. This method is described more precisely in our previous work [20].

Method 2: Ammonium bicarbonate salt Method

Carbonization of Kevlar was carried out in a smelting furnace in a combined gas atmosphere generated by using ammonium bicarbonate salt. Ammonium bicarbonate is an inorganic compound with formula NH_4HCO_3, and it decomposes when heated above 36 °C, releasing ammonia, water, and carbon dioxide gases as follows: $NH_4HCO_3 \rightarrow NH_3 + H_2O + CO_2$, so the atmosphere created inside the furnace is mainly a mixture of gasses: CO_2 and NH_3, replacing air.

The Kevlar fabric samples in rolled form, were placed inside a cylindrical crucible, positioned in the center of the furnace. A total of 10 g of ammonium bicarbonate salt was added into the crucible containing the Kevlar sample, in order to create a mixed gas atmosphere. The Kevlar fabric samples were carbonized to four final temperatures from 800 to 1100°C, with an interval of 100 °C.

Method 3: N_2 Method

Carbonization of Kevlar was carried out in a high-temperature furnace, in the presence of an inert N_2 flow atmosphere; a heating rate of 10 °C/min and holding time of 20 min at the final temperature was adopted. The Kevlar fabric samples were carbonized to four final temperatures from 800 to 1100 °C, with an interval of 100 °C.

The carbon samples obtained from the three methods mentioned above are listed in Table 1, with details of their yields in percentages. For all three methods, the final product at every selected final carbonization temperature, although weak, retained its fabric form and possessed structural integrity, making it suitable to handle for further investigations.

Table 1. Details of carbonized samples.

Sample Code	Atmosphere Type	Carbonization Method	Final Carbonization Temperature (°C)	Fabric Yield (%)	Carbon Yield (%)
C8	CO_2	1	800	58.24 ± 1.3	69.1 ± 0.9
C9	CO_2	1	900	47.26 ± 1.6	76.4 ± 1.2
C10	CO_2	1	1000	35.69 ± 2.1	83.4 ± 0.8
C11	CO_2	1	1100	31.44 ± 1.8	89.1 ± 0.4
A8	Gas mixture	2	800	30.21 ± 1.1	83.7 ± 0.6
A9	Gas mixture	2	900	26.31 ± 1.7	87.1 ± 0.6
A10	Gas mixture	2	1000	23.49 ± 2.5	88.5 ± 0.8
A11	Gas mixture	2	1100	19.89 ± 2.8	90.2 ± 0.8
N8	Nitrogen	3	800	46.23 ± 1.1	67.2 ± 0.9
N9	Nitrogen	3	900	41.79 ± 1.2	73.4 ± 0.8
N10	Nitrogen	3	1000	34.47 ± 1.9	84.1 ± 0.6
N11	Nitrogen	3	1100	30.60 ± 1.5	88.2 ± 0.8

Energy dispersive X-ray (EDX) analysis was carried out using an LZ 5 EDX detector, Oxford Instruments, High Wycombe, UK, in order to calculate the relative percentages of different elements in the activated material after the carbonization process at different temperatures. The elemental analysis of the starting material, Kevlar, in terms of weight percentages on dry basis, was 63.85% C, 15.09% N, 0.8% S, and 18.84% O [20]. Thermal degradation advances with increasing temperatures by the removal of volatile compounds. The increase in carbon content (as a percentage) is of primary importance when enhancing the electrical conductivity and Joule heating of the final product (shown in Table 1). The remaining composition of the carbon fabrics obtained after carbonization is made up of trivial amounts of impurities such as Na, K, Cl, and Ca.

2.3. Ohmic Heating Measurement

The Joule heating behavior of the carbon fabric samples were characterized using a test setup as illustrated in Figure 1. The test sample was clamped in position along its width by a pair of 6 cm long electrodes at both ends, which were 8 cm apart. These electrodes were connected to a DC power supply (TIPA PS3010), TIPA, spol. sr.o, Opava, Czech Republic. An IR camera (FLIR-E6390), Teledyne FLIR LLC, Oregon, USA. was placed above the test sample at a height of 40 mm, in order to monitor the surface temperature and heat distribution on the sample surface. The current 1 A was kept constant, and the voltage was gradually increased from 0 V to 10 V, at intervals of 1 V, with a holding time of 10 s, and the average temperature over the middle section of the material between the two sets of electrodes was considered.

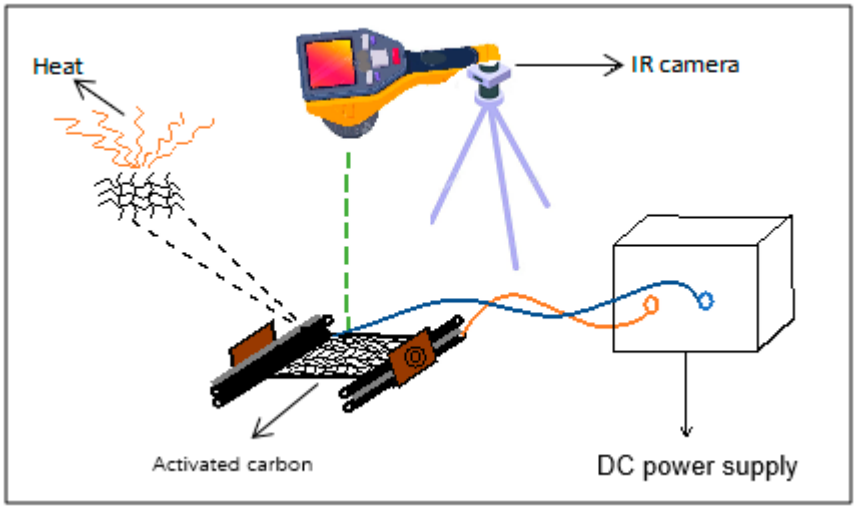

Figure 1. Joule heating measurement setup.

Furthermore, to investigate the Joule heating performance of the carbon fabrics obtained by different methods of carbonization, a constant voltage of 5 V was applied to evaluate the heating/cooling kinetics based on the time-temperature characteristics of the materials.

2.4. Electrical Resistivity

Correspondingly, the test sample was clamped the same way as mentioned in the previous section to measure the Joule heating and was connected to a digital multimeter, which displayed the electrical resistance (in ohms) of the material. A current flow of 1 A was set by regulating the voltage and the resistance value was recorded after 10 s. Furthermore, the electrical resistivity (in ohm.cm) was calculated mathematically as follows [7]:

$$\rho = \frac{A \times R}{L} \tag{2}$$

where ρ is the electrical resistivity (in ohm.cm); A is the cross-sectional area (along the width of the fabric sample in our case); R is the resistance measured (by the multimeter); and L is the length of the fabric sample.

3. Results and Discussions

3.1. Electrical Resistivity

Figure 2 shows the electrical resistivity of the fabrics carbonized to four final temperatures ranging from 800–1100 °C, using methods 1, 2, and 3. The electrical resistivity of all samples was measured five times per sample. It is evident that for all three methods, the electrical resistivity decreased progressively with increasing carbonization temperatures.

This is attributed to the higher carbon yield due to carbonization at higher temperatures, due to the removal of organic compounds in the form of volatiles [21,22]. These carbon-rich fabrics acquire a dense micro current network and create a better passage for current flow. Migration and hopping of electrons through the fibrous network, being a potential means of electron transport, is thought to be responsible for the higher electrical conductivity or lower resistivity [20,23]. For all three methods, there was no significant difference in the resistivity between fabrics carbonized at 800 °C to 1000 °C. The electrical resistivity of fabrics processed by methods 1 and 2 were nearly the same at 1000 °C and 1100 °C carbonization temperatures. Overall, in all three methods the carbonized fabrics displayed lower resistivity, or rather greater conductivity at higher carbonization temperatures, which indicates higher current flow through these materials, thus contributing to increased Joule heating.

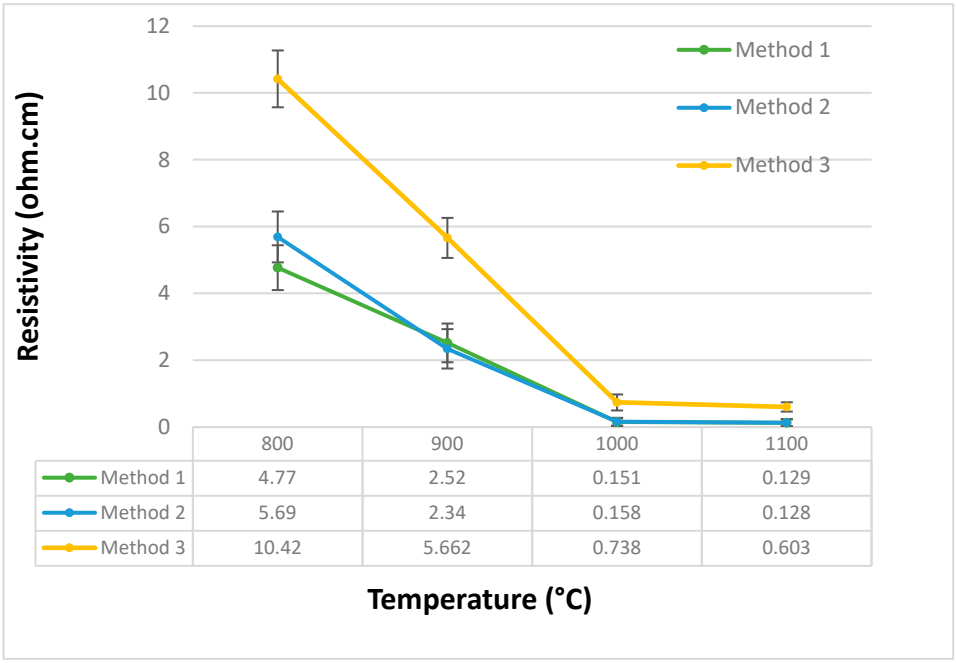

	800	900	1000	1100
Method 1	4.77	2.52	0.151	0.129
Method 2	5.69	2.34	0.158	0.128
Method 3	10.42	5.662	0.738	0.603

Figure 2. Electrical resistivity of activated carbon fabrics from methods 1, 2, and 3.

3.2. Joule Heating Characteristics

Temperature–Voltage (T-V) relation

The surface temperature of activated carbon fabrics was investigated at applied voltages ranging from 0 to 10 V, at intervals of 1 V for constant current I = 1 A; the surface temperature was recorded 10 s after setting the specific voltage. Figure 3a–c show the T–V curves of the fabrics carbonized by methods 1, 2, and 3, respectively. For each sample, the average value of five test measurements was considered. For fabrics obtained by all three methods, observations made from the T–V curves demonstrate that, initially, the surface temperatures stayed nearly the same, without a significant rise in temperature when a low voltage (V < 3 V) was supplied. Subsequently, with increasing voltage, the surface temperature of the fabrics gradually increased. Similarly, for all three methods, the fabrics carbonized at 1000 °C and 1100 °C showed a considerably steep increase in surface temperature with increasing voltage. The surface temperatures for fabrics carbonized at 1000 °C and 1100 °C were nearly alike over the entire range of applied voltage (0–10 V). At the maximum applied voltage (10 V), methods 1, 2, and 3 showed surface temperatures of 244 °C, 264 °C, and 210 °C, for fabrics carbonized at 1000 °C.

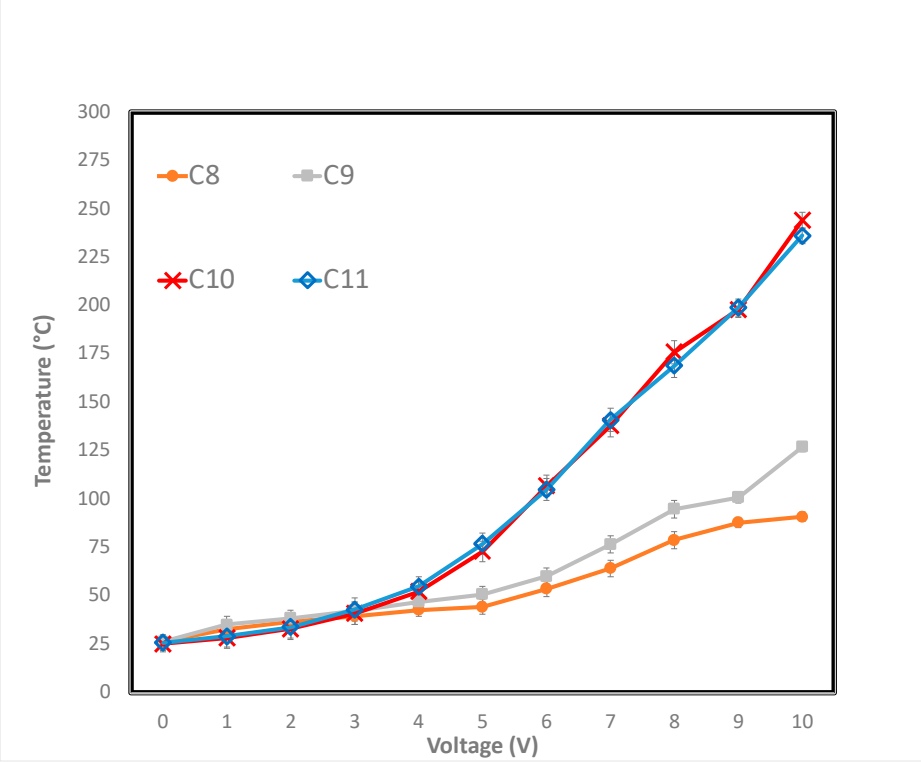

(**a**)

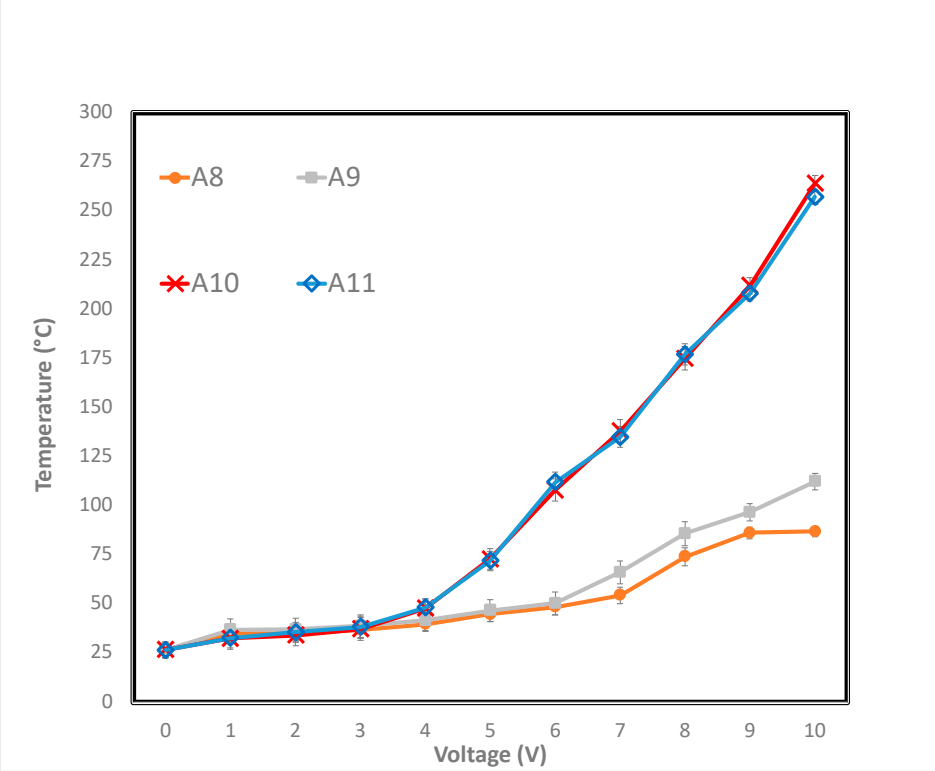

(**b**)

Figure 3. *Cont.*

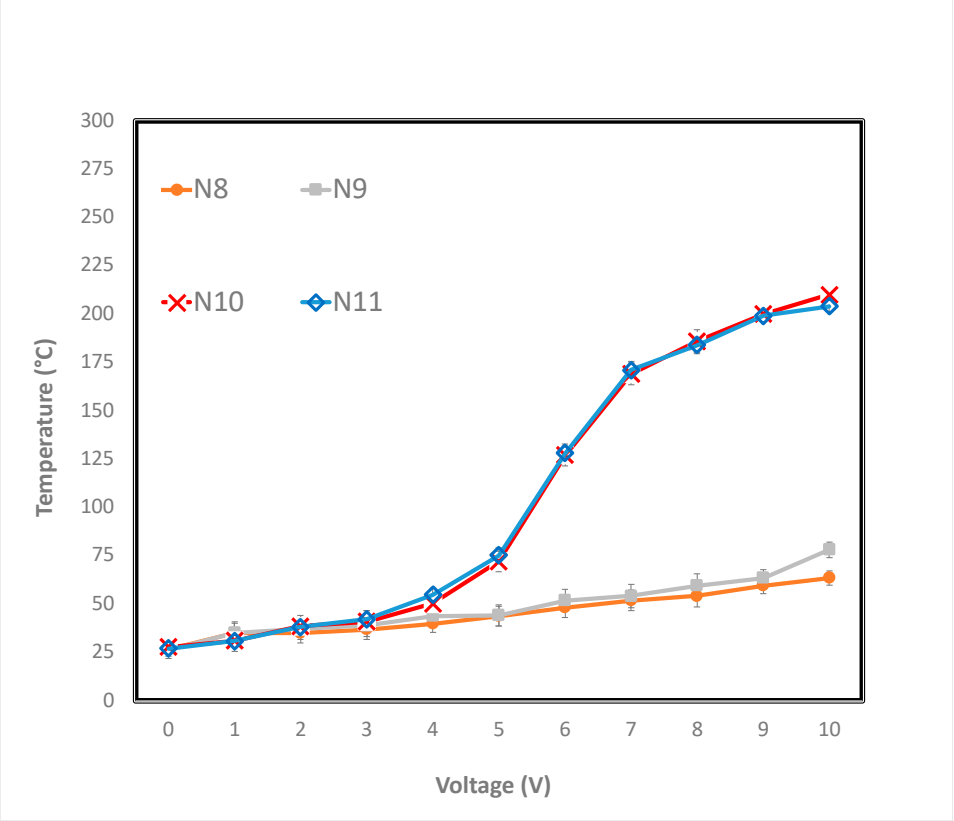

(**c**)

Figure 3. Temperature–voltage relation of activated carbon fabrics from (**a**) method 1; (**b**) method 2; and (**c**) method 3.

Heating/Cooling Kinetics: Temperature–Time (T–I) relation

The purpose of this segment was to analyze the kinetics of continuous heating and cooling of the carbon fabrics, obtained by time-dependent temperature (T–I) relation curves (shown in Figure 4). For each sample, the average value of five test measurements was considered. It is evident that for all the samples, the surface temperature increased steeply once the voltage (set at 5 V) was applied starting at 0 s, and then, after 30 s, the rate of temperature growth gradually increased and reached the maximum temperature at 120 s. Consecutively, after switching off the electrical power supply, the temperature decreased rapidly to room temperature. The stable increase in temperature by Joule heating for fabrics obtained by all three methods greatly depended on the final carbonization temperature. Furthermore, the leveling-off temperature was higher for fabrics carbonized at 1000 °C and 1100 °C, for all three methods at the same applied voltage (5 V). It is clear that under the same applied voltage, the magnitudes of the maximum temperatures were nearly the same for fabrics carbonized at 1000 °C and 1100 °C for all three methods. For this reason, the fabrics carbonized at 1000 °C, using the three methods (C10, A10, and N10), were taken into consideration for comparison (Figure 4d). The maximum temperature of C10 was slightly higher than that of A10 and N10. Furthermore, the initial increase in surface temperature with respect to time was significantly higher for C10 than for A10 and N10. This can be attributed to the more uniform distribution of graphite layers with the fibrous structures for higher current flow. The delay in the increase of surface temperature before reaching a maximum, especially for A10 and N10, is possibly be due to the initial heat loss due to convention or radiation, which means it takes longer for current to be distributed uniformly as possible, throughout the surface of the fabric, and thus takes longer to stabilize and reach the maximum temperature.

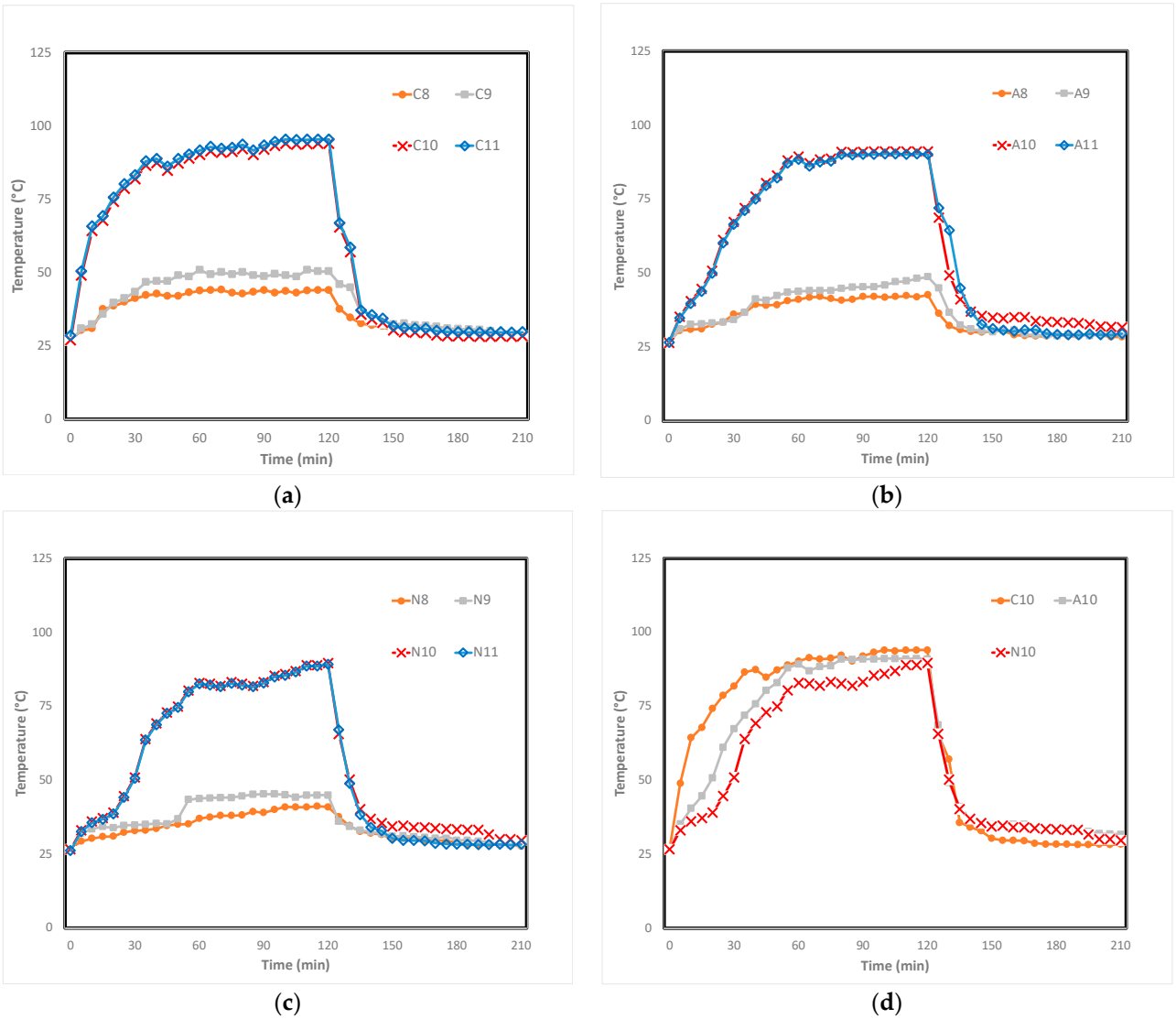

Figure 4. Temperature–time relation of activated carbon fabrics from (**a**) method 1; (**b**) method 2; (**c**) method 3; and (**d**) comparison of the three methods for fabrics carbonized at 1000 °C.

Here, three heating/cooling kinetic parameters, namely, heating time constant, efficiency of heat transfer, and cooling time constant were obtained to further investigate the Joule heating properties of the carbon fabrics. The T–I curves for fabrics obtained by all three methods shown in Figure 4 can be divided into three sections: (i) temperature growth (heating; 0–60 s), (ii) the region of equilibrium (maximum temperature; 60–120 s), and (iii) temperature decay (cooling; 120–210 s) [24,25].

The heating/cooling kinetics can be simply expressed by a rate equation of the first order, where rate of temperature change dT/dt is proportional to actual temperature T. For the heating phase, the rate equation is of the form [24,25]:

$$\frac{dT}{dt} = -k_h(T_m - T) \tag{3}$$

where T_m is maximum temperatue in equlibrium and k_h is the rate constant of heating, which is evidently replaced by the time constant $\tau_g = 1/k_h$. Integration of this differntial

equation in the range from ambient temperature T_0, at time $t = 0$, to temperature T_t, at time t, leads to the following equation [24,25]:

$$\frac{T_t - T_0}{T_m - T_0} = 1 - \exp(-t/\tau_g) \quad (4)$$

The initial heating segment is expressed by Equation (4) and the parameters T_m, τ_g are obtained by nonlinear regression.

For the cooling phase, starting from time t_0, it can be shown that [24,25]:

$$\frac{T_t - T_0}{T_m - T_0} = \exp(-(t - t_0)/\tau_d) \quad (5)$$

where cooling time constant is $\tau_d = 1/k_c$.

The resulting values for all the activated carbon fabrics are listed in Table 2. The values of τ_g for N10 and N11 are greater than those of A10, A11, C10, and C11 because of their higher resistivity.

Table 2. Characteristic parameters (τ_g, $hr+c$, and τ_d) for Joule heating performance of all activated carbon fabric samples under applied voltages.

Carbonization Method	Carbonization Temperature	τ_g (S)	h_{r+c} (W/°C)	τ_d (S)
1	800	19.60	0.09	89.83
	900	24.11	0.08	107.52
	1000	19.84	0.07	57.82
	1100	19.63	0.07	60.66
2	800	30.36	0.04	100.77
	900	41.01	0.04	126.59
	1000	25.99	0.10	92.24
	1100	28.92	0.10	89.12
3	800	44.82	0.03	126.82
	900	38.86	0.03	105.76
	1000	42.17	0.09	88.94
	1100	41.68	0.10	70.21

The τ_d values obtained from nonlinear regression of experimental time-dependent temperature decay data, using Model (5), are summarized in Table 2. The τ_g and τ_d values of C10 and C11 were noticeably lower than those of A10, A11, N10, and N11. This means that C10 and C11 exhibited comparatively more rapid temperature responses to applied voltages and were easier to control.

In the maximum temperature zone (region of equilibrium), where the temperature as a function of time becomes constant, the heat gain by electric power is counteracted by the heat emitted to the surroundings through radiation and/or convection, due to conservation of energy. As such, the heat transferred through radiation and convection, h_{r+c}, can be expressed as [24,25]:

$$h_{r+c} = \frac{I_c V_0}{T_m - T_0} \quad (6)$$

where I_c is the steady-state current and V_0 is the applied voltage. It can be seen in Table 2 that the h_{r+c} increases with A10, A11, N10, and N11 as compared to C10 and C11, indicating that comparatively more electrical energy is required to maintain the maximum temperatures for these materials. In the third segment, the material at maximum temperature is left to cool down to the ambient temperature according to Equation (5).

4. Conclusions

In this work, simple and straightforward methods to utilize textile wastes in a sustainable manner with high carbon yield, electrical conductivity and joule heating behavior has been achieved. Carbonization of industrial para-aramid fabric wastes was carried out using three unadorned and straightforward methods to produce activated carbon fabric, which was then investigated for the realization of electrical resistivity and Joule heating. Inexpensive and commonly available compounds such as charcoal and ammonium bicarbonate salt (methods 1 and 2) were utilized to potentially create an oxygen-free atmosphere inside a furnace to assist in activation during the carbonization process, in comparison to N2 gas, which was used in method 3. All three methods were shown to be effective at producing activated carbon fabrics from para-aramid. The electrical resistivity of the activated carbon fabrics processed by all three methods was shown to decrease significantly with increasing carbonization temperature. Methods 1 and 2 showed lower electrical resistivity in comparison to method 3. Both electrical resistivity and Joule heating characteristics were greatly influenced by the final carbonization temperatures for all three methods. For fabrics obtained by all three methods, it can be seen that in the T–V curves the surface temperature remained low with no significant changes when a low voltage (V < 3 V) was supplied. However, the surface temperature of the fabrics increased with higher voltage (V > 3 V). At maximum voltage (10 V), C10 and A10 showed the highest surface temperatures of 244 °C and 264 °C due to lower electrical resistivity, or greater conductivity. To further investigate the thermal properties of the carbonized materials, we expressed three heating/cooling kinetic parameters. The increase in temperature by Joule heating for fabrics obtained by all three methods greatly depended on the final carbonization temperature. The leveling-off temperature was higher for fabrics carbonized at 1000 °C and 1100 °C, for all three methods at the same applied voltage (5 V). The maximum temperature of C10 was slightly higher than that of A10 and N10. Moreover, the initial increase in surface temperature with respect to time was significantly higher for C10 than for A10 and N10. Cumulatively, we can say that methods 1 and 2, which utilized charcoal and ammonium bicarbonate salt, were comparatively more desirable in terms of both electrical and Joule heating characteristics, while also being cost-effective and sustainable. We concluded that this material retains structural integrity after carbonization at specified temperatures (800 to 1100°C), excellent electrical conductivity and Joule heating ability, and can thus be proposed as a material for protective panels, enabling EMI shielding and heat generation via external powering towards thermally and/or electrically regulated sensors.

Author Contributions: Conceptualization, D.K. and J.M.; data curation, Y.W.; formal analysis, D.K. and Y.W.; funding acquisition, M.V.; investigation, D.K.; methodology, D.K.; project administration, J.M. and M.V.; resources, Y.W. and M.V.; supervision, J.M.; visualization, D.K.; writing—original draft, D.K.; writing—review and editing, J.M. All authors have read and agreed to the published version of the manuscript.

Funding: This work was supported by the Czech Science Foundation (GACR)-project "Advanced structures for thermal insulation under extreme conditions" (Reg. No. 21-32510M).

Institutional Review Board Statement: Not applicable.

Informed Consent Statement: Not applicable.

Data Availability Statement: Additional details of the experiments and data may be asked via email to the corresponding author.

Conflicts of Interest: The authors declare no conflict of interest.

References

1. Kim, M.; Sung, D.H.; Kong, K.; Kim, N.; Kim, B.-J.; Park, H.W.; Park, Y.-B.; Jung, M.; Lee, S.H.; Kim, S.G. Characterization of resistive heating and thermoelectric behavior of discontinuous carbon fiber-epoxy composites. *Compos. Part B Eng.* **2016**, *90*, 37–44. [CrossRef]
2. Zhang, Q.; Yu, Y.; Yang, K.; Zhang, B.; Zhao, K.; Xiong, G.; Zhang, X. Mechanically robust and electrically conductive graphene-paper/glass-fibers/epoxy composites for stimuli-responsive sensors and Joule heating deicers. *Carbon* **2017**, *124*, 296–307. [CrossRef]
3. Isaji, S.; Bin, Y.; Matsuo, M. Electrical conductivity and self-temperature-control heating properties of carbon nanotubes filled polyethylene films. *Polymer* **2009**, *50*, 1046–1053. [CrossRef]
4. Lopes, H.; Ribeiro, J.E. Structural Health Monitoring in Composite Automotive Elements. In *New Advances in Vehicular Technology and Automotive Engineering*; Carmo, J., Ed.; InTech: London, UK, 2012. [CrossRef]
5. Zanjani, J.S.M.; Okan, B.S.; Pappas, P.-N.; Galiotis, C.; Menceloglu, Y.Z.; Yildiz, M. Tailoring viscoelastic response, self-heating and deicing properties of carbon-fiber reinforced epoxy composites by graphene modification. *Compos. Part A Appl. Sci. Manuf.* **2018**, *106*, 1–10. [CrossRef]
6. Athanasopoulos, N.; Kostopoulos, V. Resistive heating of multidirectional and unidirectional dry carbon fibre preforms. *Compos. Sci. Technol.* **2012**, *72*, 1273–1282. [CrossRef]
7. Redondo, O.; Prolongo, S.; Campo, M.; Sbarufatti, C.; Giglio, M. Anti-icing and de-icing coatings based Joule's heating of graphene nanoplatelets. *Compos. Sci. Technol.* **2018**, *164*, 65–73. [CrossRef]
8. Jiménez, V.; Sánchez, P.; Romero, A. Materials for activated carbon fiber synthesis. In *Activated Carbon Fiber and Textiles*; Woodhead Publishing: Sawston, UK, 2017; pp. 21–38. [CrossRef]
9. Ko, K.S.; Park, C.W.; Yoon, S.-H.; Oh, S.M. Preparation of Kevlar-derived carbon fibers and their anodic performances in Li secondary batteries. *Carbon* **2001**, *39*, 1619–1625. [CrossRef]
10. Mosquera, M.E.; Jamond, M.; Martinez-Alonso, A.; Tascon, J.M. Thermal Transformations of Kevlar Aramid Fibers During Pyrolysis: Infrared and Thermal Analysis Studies. *Chem. Mater.* **2002**, *6*, 1918–1924. Available online: https://pubs.acs.org/doi/pdf/10.1021/cm00047a006 (accessed on 5 October 2021). [CrossRef]
11. Yang, M.; Zhu, X.L.; Liang, G. Pyrolysis Process of Kevlar Fibers with Thermogravimetric Analysis coupled and Fourier Transform Infrared Spectroscopy. *Guang Pu* **2016**, *36*, 1374–1377. [PubMed]
12. Ramgobin, A.; Fontaine, G.; Bourbigot, S. Thermal Degradation and Fire Behavior of High Performance Polymers. *Polym. Rev.* **2019**, *59*, 55–123. [CrossRef]
13. Chen, J.; Harrison, I. Modification of polyacrylonitrile (PAN) carbon fiber precursor via post-spinning plasticization and stretching in dimethyl formamide (DMF). *Carbon* **2002**, *40*, 25–45. [CrossRef]
14. EFitzer, E.; Frohs, W.; Heine, M. Optimization of stabilization and carbonization treatment of PAN fibres and structural characterization of the resulting carbon fibres. *Carbon* **1986**, *24*, 387–395. [CrossRef]
15. Edie, D.D. The effect of processing on the structure and properties of carbon fibers. *Carbon* **1998**, *36*, 345–362. [CrossRef]
16. Huang, X. Fabrication and Properties of Carbon Fibers. *Materials* **2009**, *2*, 2369–2403. [CrossRef]
17. Chen, J.Y. *Activated Carbon Fiber and Textiles*; Woodhead Publishing: Sawston, UK, 2016; p. 342.
18. Choma, J.; Osuchowski, L.; Marszewski, M.; Dziura, A.; Jaroniec, M. Developing microporosity in Kevlar®-derived carbon fibers by CO_2 activation for CO_2 adsorption. *J. CO2 Util.* **2016**, *16*, 17–22. [CrossRef]
19. Brown, J.R.; Power, A.J. Thermal degradation of aramids: Part I—Pyrolysis/gas chromatography/mass spectrometry of poly(1,3-phenylene isophthalamide) and poly(1,4-phenylene terephthalamide). *Polym. Degrad. Stab.* **1982**, *4*, 379–392. [CrossRef]
20. Karthik, D.; Baheti, V.; Militky, J.; Naeem, M.S.; Tunakova, V.; Ali, A. Activated Carbon Derived from Carbonization of Kevlar Waste Materials: A Novel Single Stage Method. *Materials* **2021**, *14*, 6433. [CrossRef] [PubMed]
21. Suárez-García, F.; Martinez-Alonso, A.; Tascón, J.M. Activated carbon fibers from Nomex by chemical activation with phosphoric acid. *Carbon* **2004**, *42*, 1419–1426. [CrossRef]
22. Conte, G.; Stelitano, S.; Policicchio, A.; Minuto, F.D.; Lazzaroli, V.; Galiano, F.; Agostino, R.G. Assessment of activated carbon fibers from commercial Kevlar® as nanostructured material for gas storage: Effect of activation procedure and adsorption of CO_2 and CH_4. *J. Anal. Appl. Pyrolysis* **2020**, *152*, 104974. [CrossRef]
23. Naeem, S.; Baheti, V.; Tunakova, V.; Militky, J.; Karthik, D.; Tomkova, B. Development of porous and electrically conductive activated carbon web for effective EMI shielding applications. *Carbon* **2017**, *111*, 439–447. [CrossRef]
24. El-Tantawy, F.; Kamada, K.; Ohnabe, H. In situ network structure, electrical and thermal properties of conductive epoxy resin–carbon black composites for electrical heater applications. *Mater. Lett.* **2002**, *56*, 112–126. [CrossRef]
25. Kong, K.; Deka, B.K.; Kim, M.; Oh, A.; Kim, H.; Park, Y.-B.; Park, H.W. Interlaminar resistive heating behavior of woven carbon fiber composite laminates modified with ZnO nanorods. *Compos. Sci. Technol.* **2014**, *100*, 83–91. [CrossRef]